

LHC HIGGS CROSS SECTION WORKING GROUP*

PUBLIC NOTE

**Constraining EFT parameters using simplified template
cross sections**

C. Hays^{1,†}, V. Sanz^{2,‡}, and G. Zemaityte^{1,§}

¹ *University of Oxford,
Oxford OX1 3RH, United Kingdom*

² *University of Sussex,
Brighton BN1 9RH, United Kingdom*

* <https://twiki.cern.ch/twiki/bin/view/LHCPhysics/LHCHXSWG>

† chris.hays@physics.ox.ac.uk

‡ v.sanz@sussex.ac.uk

§ gabija.zemaityte@physics.ox.ac.uk

Abstract

We discuss a procedure for fitting a set of dimension-6 effective field theory parameters using simplified template cross section measurements. The steps are to determine equations relating the parameters to the cross sections, choose the fit parameters and external constraints, and perform the fit. In this example the equations are calculated using the HEL model in the Madgraph generator, which is a partial implementation of the SILH basis at leading order in perturbation theory.

1 Introduction

Following the Run 1 discovery of the Higgs boson [1, 2] and the verification of its interactions with SM particles, several frameworks have been defined [3] to probe the production and decay of the Higgs boson in more detail. Two examples are the simplified template cross sections (STXS), which measure production rates in various kinematic regions, and effective field theories (EFT), which extend the SM Lagrangian to higher order in a momentum expansion in order to parameterize the effects of possible new processes. In this note we describe procedures for performing a fit to a set of EFT parameters using STXS measurements as input.

The fit described in this note, and labelled as a stage-1 fit, should be understood as a *proof-of-concept* description which can then be improved in subsequent stages. There are several steps to the fit: first, we define the parameter set for the fit, including any assumptions or constraints from external measurements (Section 2); next, we determine the relations between the STXS measurements and the EFT parameters (Section 3); and finally, we discuss the likelihood fit to the STXS measurements (Section 4).

2 Parameters and constraints

We use the Higgs Effective Lagrangian (HEL) implementation of 39 flavour-independent dimension-6 operators in Feynrules and Madgraph described in Ref. [4]. The operators

and coefficients are shown in Tables 1 and 2, along with current constraints from Run-1 Higgs and diboson measurements, electroweak precision measurements, and multijet measurements. The parameters in text font (e.g. cG) correspond to the variable definitions in the Feynrules model implementation. The SM parameters in the HEL model are $m_W = 80.385$ GeV, $G_F = 1.16637 \times 10^{-5}$ GeV⁻², $v = (2G_F^2)^{-1/4} = 246$ GeV, $g = 2m_W/v = 0.653$, $\alpha_{EM} = e^2/(4\pi) = 1/127.9$, $\sin\theta_W = e/g = 0.48$, $g' = e/\cos\theta_W = 0.357$, and $\alpha_s = g_s^2/(4\pi) = 0.1184$. The electroweak scheme takes m_W , α_{EM} , and G_F as inputs and calculates m_Z ¹. Note that only 37 of the operators in HEL are linearly independent due to the following relationship between the model parameters [4]: $\mathcal{O}_B = 2 \tan^2\theta_W (\sum_\psi Y_\psi \mathcal{O}_{H\psi} - \mathcal{O}_T)$, and $\mathcal{O}_W = -2\mathcal{O}_H + \frac{4}{v^2} H^\dagger H D^\mu H^\dagger D_\mu H + \mathcal{O}'_{HQ} + \mathcal{O}'_{HL}$.

The operators sensitive to Higgs boson production and decay include those involving the effective Hgg and $H\gamma\gamma$ vertices \mathcal{O}_g and \mathcal{O}_γ , respectively, along with their CP-violating counterparts $\tilde{\mathcal{O}}_g$ and $\tilde{\mathcal{O}}_\gamma$. These operators are constrained by gluon fusion production and by Higgs-boson decay to diphotons [6]. Constraints on the CP-odd operators have only been derived using CP-even measurements that have sensitivity at $\mathcal{O}(1/\Lambda^4)$. The constraints assume that these are the only non-zero operators [7]; they are given in Table 1.

The Yukawa-type flavour-independent operators involving Hff interactions are \mathcal{O}_u , \mathcal{O}_d , and \mathcal{O}_ℓ , affecting $t\bar{t}H$, $H \rightarrow b\bar{b}$, and $H \rightarrow \tau\tau$ processes, respectively. These are taken to be real in the HEL model, so CP-odd contributions are not considered here. Operators involving only the Higgs field, \mathcal{O}_H and \mathcal{O}_6 , affect the Higgs-field normalization and the Higgs self-coupling, respectively. These are not well constrained: the Higgs-field normalization produces a global scaling of SM Higgs couplings, so it is correlated with many other operators; and experimental sensitivity to the Higgs pair-production cross section is an order of magnitude higher than the SM prediction.

Operators affecting Higgs boson interactions with weak bosons include \mathcal{O}_{HW} , \mathcal{O}_{HB} , \mathcal{O}_W , and \mathcal{O}_B . Measurements of VBF and VH production, and of $H \rightarrow VV$ decay, constrain the first two operators and the combination $\mathcal{O}_W - \mathcal{O}_B$. The combination $\mathcal{O}_W + \mathcal{O}_B$ is related to the Peskin-Takeuchi S parameter [8] that is tightly constrained by electroweak precision measurements. The operator \mathcal{O}_{3W} is constrained by diboson production and by VBF production of a single weak boson. Constraints on the corresponding CP-violating operators $\tilde{\mathcal{O}}_{HW}$, $\tilde{\mathcal{O}}_{HB}$, and $\tilde{\mathcal{O}}_{3W}$ have been obtained assuming other operators are zero; Table 1 shows the constraints from Ref. [7].

Other operators enter Higgs boson production and decay but are tightly constrained by precision electroweak and QCD data. The operator \mathcal{O}_T is related to the Peskin-

¹In other implementations of the EFT Lagrangian, the measurement of the Z -boson mass m_Z is instead used as an input, as well as α from the low-energy limit of Compton scattering and G_F from the muon decay. Moreover, there is a further set of choices to be made when dealing with the kinetic mixing between the photon and Z boson induced by the EFT operators. These sets of prescriptions are described in e.g. the NLO version of the HEL Lagrangian [5].

Table 1: The dimension-6 HEL operators affecting Higgs boson production, and the 95% confidence level constraints on the coefficients expressed in terms of the HEL parameters (shown in monospace font). We denote with the symbol \times the operators which are not currently bounded.

HEL operator	Coefficient	HEL constraint
$\mathcal{O}_g = H ^2 G_{\mu\nu}^A G^{A\mu\nu}$	$\frac{c_g}{\Lambda^2} = \frac{g_s^2}{m_W^2} \mathbf{cG}$	$-3.2 < \mathbf{cG}/10^{-4} < 1.1$
$\tilde{\mathcal{O}}_g = H ^2 G_{\mu\nu}^A \tilde{G}^{A\mu\nu}$	$\frac{c_{\tilde{g}}}{\Lambda^2} = \frac{g_s^2}{m_W^2} \mathbf{tcG}$	$ \mathbf{tcG} < 1.2 \times 10^{-4}$
$\mathcal{O}_\gamma = H ^2 B_{\mu\nu} B^{\mu\nu}$	$\frac{c_\gamma}{\Lambda^2} = \frac{g'^2}{m_W^2} \mathbf{cA}$	$-11 < \mathbf{cA}/10^{-4} < 2.2$
$\tilde{\mathcal{O}}_\gamma = H ^2 B_{\mu\nu} \tilde{B}^{\mu\nu}$	$\frac{c_{\tilde{\gamma}}}{\Lambda^2} = \frac{g'^2}{m_W^2} \mathbf{tcA}$	$ \mathbf{tcA} < 12 \times 10^{-4}$
$\mathcal{O}_u = y_u H ^2 \bar{Q}_L H^\dagger u_R + \text{h.c.}$	$\frac{c_u}{\Lambda^2} = -\frac{\mathbf{cu}}{v^2}$	$-0.084 < \mathbf{cu} < 0.155$
$\mathcal{O}_d = y_d H ^2 \bar{Q}_L H d_R + \text{h.c.}$	$\frac{c_d}{\Lambda^2} = -\frac{\mathbf{cd}}{v^2}$	$-0.198 < \mathbf{cd} < 0.088$
$\mathcal{O}_\ell = y_\ell H ^2 \bar{L}_L H \ell_R + \text{h.c.}$	$\frac{c_\ell}{\Lambda^2} = -\frac{\mathbf{cl}}{v^2}$	\times
$\mathcal{O}_H = (\partial^\mu H ^2)^2$	$\frac{c_H}{\Lambda^2} = \frac{\mathbf{cH}}{2v^2}$	$-0.14 < \mathbf{cH} < 0.194$
$\mathcal{O}_6 = (H^\dagger H)^3$	$\frac{c_6}{\Lambda^2} = -\frac{\lambda}{v^2} \mathbf{c6}$	\times
$\mathcal{O}_{HW} = i (D^\mu H)^\dagger \sigma^a (D^\nu H) W_{\mu\nu}^a$	$\frac{c_{HW}}{\Lambda^2} = \frac{2g}{m_W^2} \mathbf{cHW}$	$-0.035 < \mathbf{cHW} < 0.015$
$\tilde{\mathcal{O}}_{HW} = i (D^\mu H)^\dagger \sigma^a (D^\nu H) \tilde{W}_{\mu\nu}^a$	$\frac{c_{\tilde{H}\tilde{W}}}{\Lambda^2} = \frac{g}{m_W^2} \mathbf{tcHW}$	$ \mathbf{tcHW} < 0.060$
$\mathcal{O}_{HB} = i (D^\mu H)^\dagger (D^\nu H) B_{\mu\nu}$	$\frac{c_{HB}}{\Lambda^2} = \frac{g'}{m_W^2} \mathbf{cHB}$	$-0.045 < \mathbf{cHB} < 0.075$
$\tilde{\mathcal{O}}_{HB} = i (D^\mu H)^\dagger (D^\nu H) \tilde{B}_{\mu\nu}$	$\frac{c_{\tilde{H}\tilde{B}}}{\Lambda^2} = \frac{g'}{m_W^2} \mathbf{tcHB}$	$ \mathbf{tcHB} < 0.24$
$\mathcal{O}_W = i \left(H^\dagger \sigma^a \overleftrightarrow{D}^\mu H \right) D^\nu W_{\mu\nu}^a$	$\frac{c_W}{\Lambda^2} = \frac{g}{m_W^2} \mathbf{cWW}$	$-0.035 < \mathbf{cWW} - \mathbf{cB} < 0.005$
$\mathcal{O}_B = i \left(H^\dagger \overleftrightarrow{D}^\mu H \right) \partial^\nu B_{\mu\nu}$	$\frac{c_B}{\Lambda^2} = \frac{g'}{2m_W^2} \mathbf{cB}$	$-0.0033 < \mathbf{cWW} + \mathbf{cB} < 0.0018$

Takeuchi T parameter [8]. Forward-backward asymmetry measurements [9] constrain operators with Vff interactions: \mathcal{O}_R^u , \mathcal{O}_R^d , \mathcal{O}_R^e , \mathcal{O}_L^q , and $\mathcal{O}_L^{(3)q}$. Finally, the operator affecting the triple-gluon vertex, \mathcal{O}_{3G} , is constrained by multijet measurements [10]. The \mathcal{O}_{2G} operator has not been constrained using this basis but is expected to be more strongly constrained [11]; to be conservative we quote the same 95% C.L. limits for \mathcal{O}_{3G} and \mathcal{O}_{2G} in the table.

Eleven operators in the HEL implementation are not shown in Tables 1 and 2, as they have not been included in previous fits. Nine of these affect couplings between fermions and gauge bosons, and two are linearly dependent on the other operators.

Table 2: The dimension-6 HEL operators affecting electroweak and QCD processes, and the constraints on the coefficients expressed in terms of the HEL parameters (shown in monospace font). The constraints on $c_{3\tilde{G}}$ and c_{2G} are taken to be the same as c_{3G} , since they are expected to be similar. We denote with the symbol \times the operators which are not currently bounded.

HEL operator	Coefficient	Constraint (TeV ⁻²)
$\mathcal{O}_{3W} = \epsilon_{ijk} W_{\mu\nu}^i W_{\rho}^{\nu j} W^{\rho\mu k}$	$\frac{c_{3W}}{\Lambda^2} = \frac{g_s^3}{m_W^2} \mathbf{c3W}$	$-0.083 < \mathbf{c3W} < 0.045$
$\tilde{\mathcal{O}}_{3W} = \epsilon_{ijk} W_{\mu\nu}^i W_{\rho}^{\nu j} \tilde{W}^{\rho\mu k}$	$\frac{c_{3\tilde{W}}}{\Lambda^2} = \frac{g_s^3}{m_W^2} \mathbf{tc3W}$	$ \mathbf{tc3W} < 0.18$
$\mathcal{O}_T = \left(H^\dagger \overleftrightarrow{D}^\mu H \right)^2$	$\frac{c_T}{\Lambda^2} = \frac{\mathbf{cT}}{2v^2}$	$-0.0043 < \mathbf{cT} < 0.0033$
$\mathcal{O}_{2W} = D^\mu W_{\mu\nu}^k D_\rho W_k^{\rho\nu}$	$\frac{c_{2W}}{\Lambda^2} = \frac{1}{m_W^2} \mathbf{c2W}$	\times
$\mathcal{O}_{2B} = \partial^\mu B_{\mu\nu} \partial_\rho B^{\rho\nu}$	$\frac{c_{2B}}{\Lambda^2} = \frac{1}{m_W^2} \mathbf{c2B}$	\times
$\mathcal{O}_R^u = \left(iH^\dagger \overleftrightarrow{D}_\mu H \right) (\bar{u}_R \gamma^\mu u_R)$	$\frac{c_R^u}{\Lambda^2} = \frac{\mathbf{cHu}}{v^2}$	$ \mathbf{cHu} < 0.011$
$\mathcal{O}_R^d = \left(iH^\dagger \overleftrightarrow{D}_\mu H \right) (\bar{d}_R \gamma^\mu d_R)$	$\frac{c_R^d}{\Lambda^2} = \frac{\mathbf{cHd}}{v^2}$	$-0.042 < \mathbf{cHd} < 0.0044$
$\mathcal{O}_R^e = \left(iH^\dagger \overleftrightarrow{D}_\mu H \right) (\bar{e}_R \gamma^\mu e_R)$	$\frac{c_R^e}{\Lambda^2} = \frac{\mathbf{cHe}}{v^2}$	$-0.0018 < \mathbf{cHe} < 0.00025$
$\mathcal{O}_L^q = \left(iH^\dagger \overleftrightarrow{D}_\mu H \right) (\bar{Q}_L \gamma^\mu Q_L)$	$\frac{c_L^q}{\Lambda^2} = \frac{\mathbf{cHQ}}{v^2}$	$-0.0019 < \mathbf{cHQ} < 0.0069$
$\mathcal{O}_L^{(3)q} = \left(iH^\dagger \sigma^a \overleftrightarrow{D}_\mu H \right) (\bar{Q}_L \sigma^a \gamma^\mu Q_L)$	$\frac{c_L^{(3)q}}{\Lambda^2} = \frac{\mathbf{cpHQ}}{v^2}$	$ \mathbf{cpHQ} < 0.0044$
$\mathcal{O}_{3G} = f_{abc} G_{\mu\nu}^a G_{\rho}^{\nu b} G^{\rho\mu c}$	$\frac{c_{3G}}{\Lambda^2} = \frac{g_s^3}{m_W^2} \mathbf{c3G}$	$ \mathbf{c3G} < 0.00016$
$\tilde{\mathcal{O}}_{3G} = f_{abc} G_{\mu\nu}^a G_{\rho}^{\nu b} \tilde{G}^{\rho\mu c}$	$\frac{c_{3\tilde{G}}}{\Lambda^2} = \frac{g_s^3}{m_W^2} \mathbf{tc3G}$	$ \mathbf{tc3G} < 0.00016$
$\mathcal{O}_{2G} = D^\mu G_{\mu\nu}^a D_\rho G_a^{\rho\nu}$	$\frac{c_{2G}}{\Lambda^2} = \frac{1}{m_W^2} \mathbf{c2G}$	$ \mathbf{c2G} < 0.00016$

3 Equations relating STXS to EFT parameters

We use a general set of equations relating the stage-1 STXS measurements to the SM EFT parameters, and use a Monte Carlo calculation to determine the coefficients. The equations are derived using the HEL model, which is an implementation of flavour-independent operators in the SILH basis. The STXS measurements are $\sigma_i \times \mathcal{B}_{4\ell}$, where i is a kinematic region of a specified production process (gluon fusion, vector-boson fusion, VH , ttH , tH , and bbH), and $\mathcal{B}_f/\mathcal{B}_{4\ell}$, where f is a Higgs-boson decay channel. Each STXS region is modelled using the Madgraph generator, with Pythia showering, and production regions are selected using the Rivet routine provided by the LHC

Higgs Working Group [12]. The Madgraph events are generated at leading order in perturbation theory, and the impact of each parameter is expressed as a ratio with respect to the SM prediction. This ratio will in general receive corrections from higher-order perturbative diagrams, and this can be studied in the HEL model for specific processes [5, 19].

Defining each production process as in the STXS framework, the EFT parameters are varied to determine the change in each cross section and partial width. A given cross section can be expressed in the form,

$$\sigma_{EFT} = \sigma_{SM} + \sigma_{int} + \sigma_{BSM}. \quad (1)$$

We express the non-SM contributions as fractional corrections to the SM,

$$\begin{aligned} \frac{\sigma_{int}}{\sigma_{SM}} &= \sum_i A_i c_i, \\ \frac{\sigma_{BSM}}{\sigma_{SM}} &= \sum_{ij} B_{ij} c_i c_j, \end{aligned} \quad (2)$$

where c_i are the HEL parameters and A_i and B_{ij} are coefficients derived using Madgraph. The c_i parameters can be translated to the Wilson coefficients using Tables 1 and 2. The leading term in the EFT expansion is the interference term; here we keep also the SM-independent term since it can be the leading term when the interference is small (e.g. due to symmetries). In such cases the suppression-scale dependence is the same as that of the interference terms with a dimension-8 vertex or two dimension-6 vertices; in an EFT fit one would want to estimate the effects of dimension-8 terms when the SM-independent term is dominant. To perform a fit without SM-independent terms one can simply set $B_{ij} = 0$.

The partial widths are parametrized in the same way as the cross sections ($\sigma \rightarrow \Gamma$), with the ratios of partial widths expressed as

$$\begin{aligned} \mathcal{B}_{4\ell} = \frac{\Gamma_{4\ell}}{\sum_f \Gamma_f} &\approx \frac{\Gamma_{4\ell}^{SM}}{\sum_f \Gamma_f^{SM}} \left[1 + \sum_i A_i^{4\ell} c_i + \sum_{ij} B_{ij}^{4\ell} c_i c_j - \sum_f \left(\sum_i A_i^f c_i + \sum_{ij} B_{ij}^f c_i c_j \right) \right], \\ \frac{\Gamma_f}{\Gamma_{4\ell}} &\approx \frac{\Gamma_f^{SM}}{\Gamma_{4\ell}^{SM}} \left[1 + \sum_i A_i^f c_i + \sum_{ij} B_{ij}^f c_i c_j - \left(\sum_i A_i^{4\ell} c_i + \sum_{ij} B_{ij}^{4\ell} c_i c_j \right) \right]. \end{aligned} \quad (3)$$

Here we neglect cross-terms of the form $A^{4\ell} A^f$ since they are subleading compared to the individual A terms. The $H \rightarrow 4\ell$ process is defined as $H \rightarrow ZZ^* \rightarrow 4\ell$, i.e. we neglect diagrams with intermediate photons that are typically suppressed by the experimental acceptance.

To determine the A and B coefficients, the Madgraph options `NP^2 == 1` and `NP^2 == 2` are used. The former option directly provides the interference term for each EFT parameter; the latter provides the BSM terms for individual parameters and combinations of parameters, from which the cross-terms B_{ij} ($i \neq j$) can be derived.

Since the equations are calculated at leading order, we only list terms whose A or B coefficient is $> 0.1\%$ times that of the leading corresponding A or B coefficient. These terms could be relevant in a next-to-leading order calculation where corrections with $1/(16\pi)^2$ factors are included, or if the leading term is smaller than this factor for other reasons. We round the coefficients to the second significant digit to reflect their approximate accuracy considering both the Madgraph and perturbative precisions. The complete set of terms are available on the LHC Higgs WG2 twiki [13].

The equations for the production cross sections are shown in Tables 3 to 11, and those for the partial widths in Table 12. For the loop-level effective $H\gamma\gamma$ and Hgg couplings we multiply the coefficients by $(16\pi)^2$ so that they are of the same order as the other coefficients, i.e. we define the interference factor as $A_g(16\pi^2 cG) = A_g c'_g$, and similarly for c'_γ and the corresponding CP-odd coefficients $c'_{\tilde{\gamma}}$ and c'_g .

In the leading-order HEL implementation, gluon-fusion production does not resolve the top-quark loop and is not sensitive to `cu`. Including the sensitivity to this operator and its dependence on Higgs-boson p_T is considered a high priority for future implementations.

4 Fit procedure

To provide an example of applying the equations to an STXS measurement, we demonstrate a fit to the recent ATLAS STXS measurements [14] that merge the stage 1 regions into 11 bins. With this set of combined $H \rightarrow \gamma\gamma$ and $H \rightarrow 4\ell$ measurements, we are able to simultaneously fit the following five HEL parameters: `cG`, `cA`, `cu`, `cHW`, and `cWW - cB`. We choose this parameter set since these are the leading coefficients for the measured processes that are not tightly constrained by other data. A recent ATLAS note [15] presented results with the same data set but including the `cHB` parameter, since the fit used more fine-grained data categories that separate WH and ZH production. The results we obtain for the other parameters are similar to those from ATLAS, suggesting that the SM templates used for the ATLAS STXS measurements do not significantly affect the EFT parameter dependence.

In performing the fit we use the central values and uncertainties of the STXS measurements, as well as the correlation matrix. One STXS region was poorly constrained and its correlation was not given; we assume zero correlation between this measurement and the others. The result of the fit is shown in Fig. 1 and the likelihoods are given in Fig. 2. The fit quality is good and the ATLAS results substantially tighten the

Fit to ATLAS STXS measurements (ATLAS-CONF-2017-047)

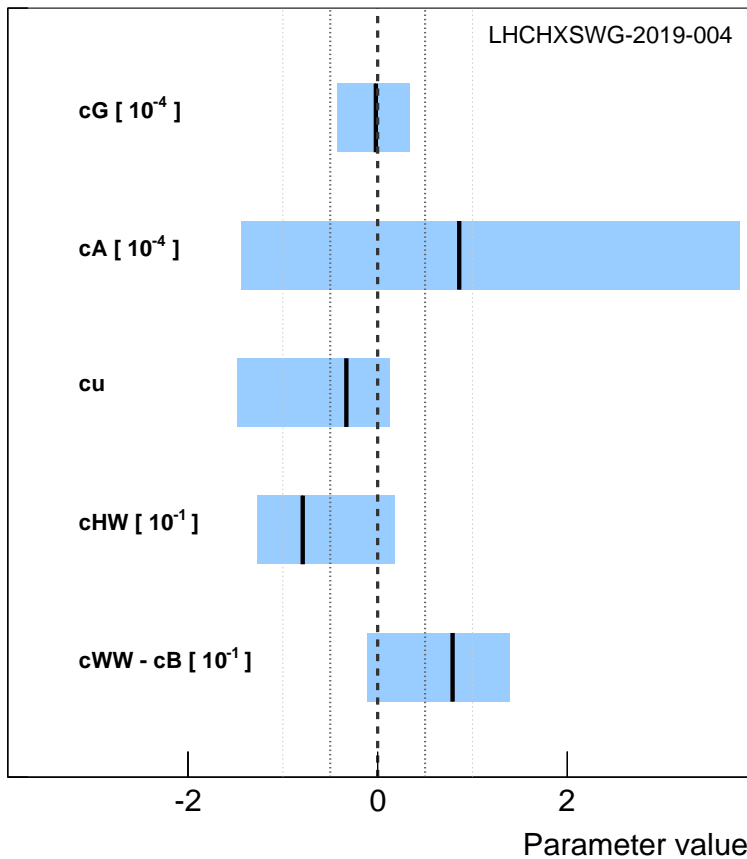


Figure 1: The best-fit values and 68% C.L. intervals for each of the five fit parameters.

constraint on cG in particular (though the results are not directly comparable to those in Table 1 since they use a different parameter set). We have obtained these results by setting all other operators to zero, while a complete EFT fit would include more datasets and fit all operators simultaneously.

5 Summary

We have described a general procedure for using the STXS framework to constrain EFT parameters, providing a first step towards the use of STXS in the context of the EFT approach. There are a number of possible theoretical improvements with the

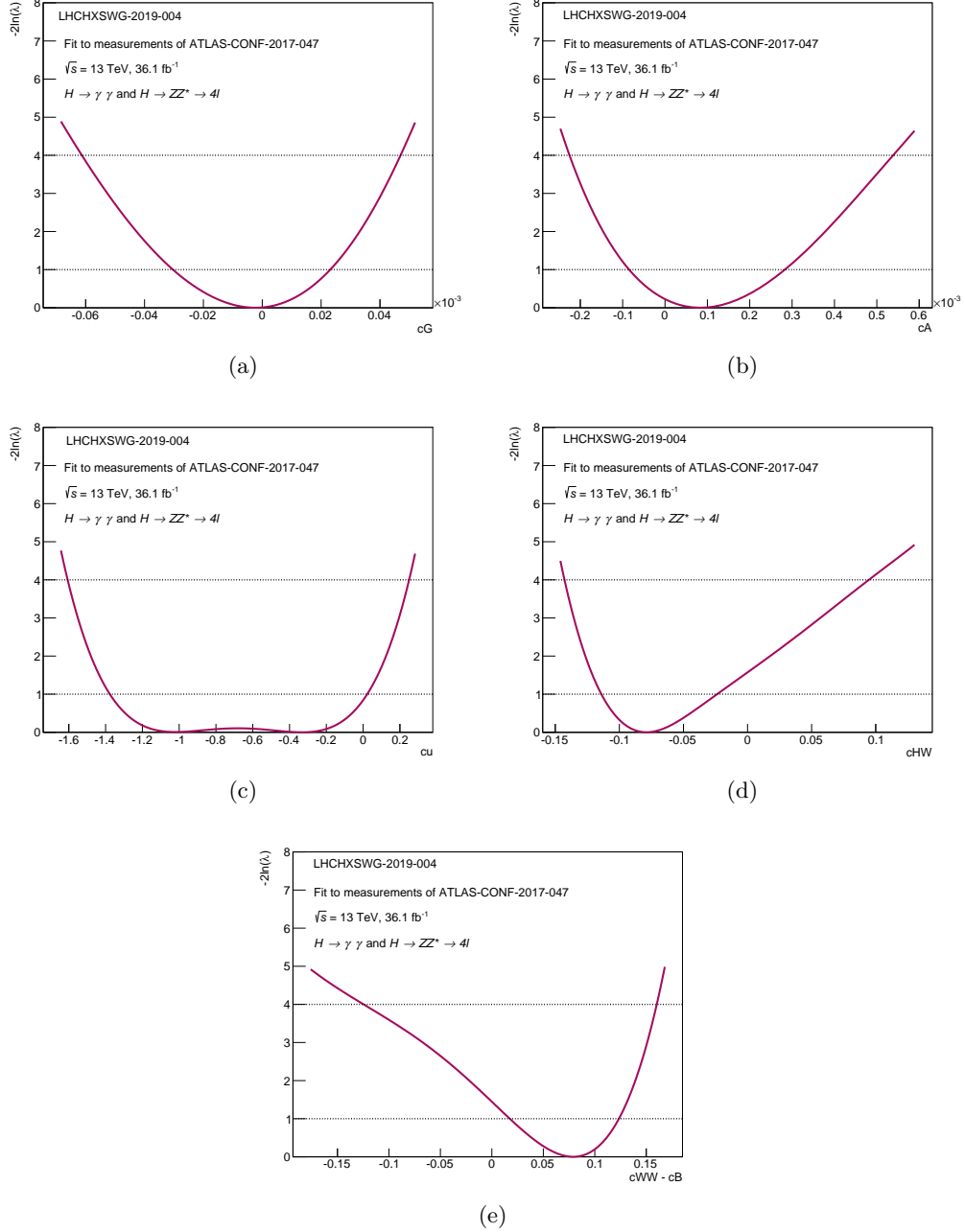


Figure 2: The observed (solid) and SM expected (dashed) profiled negative log-likelihood scans for the five-parameter fit. The parameters are (a) cG , (b) cA , (c) cu , (d) cHW , and (e) $cWW - cB$.

currently available tools and calculations: 1.) similar equations can be derived using the recent SMEFT Feynrules implementation [16] that uses the Warsaw basis [17]; 2.) the results could be expressed in terms of other bases, including the Warsaw basis, using the tool Rosetta [18]; 3.) the theoretical predictions and simulation of kinematic distributions of some Higgs operators could be performed at NLO in QCD using public implementations of the HEL Lagrangian in aMC@NLO [5] and POWHEG-BOX [19]; 4.) NLO electroweak corrections in decays could be included by interfacing with eHDECAY [20], with the use of Rosetta; and 5.) a combination with electroweak diboson production could be incorporated within the same framework.

References

- [1] ATLAS Collaboration, *Observation of a new particle in the search for the Standard Model Higgs boson with the ATLAS detector at the LHC*, Phys. Lett. B **716** (2012) 1, [arXiv:1207.7214 \[hep-ex\]](#).
- [2] CMS Collaboration, *Observation of a new boson at a mass of 125 GeV with the CMS experiment at the LHC*, Phys. Lett. B **716** (2012) 30, [arXiv:1207.7235 \[hep-ex\]](#).
- [3] LHC Higgs Cross Section Working Group, D. de Florian et al., *Handbook of LHC Higgs Cross Sections: 4. Deciphering the Nature of the Higgs Sector*, [arXiv:1610.07922 \[hep-ph\]](#).
- [4] A. Alloul, B. Fuks, and V. Sanz, *Phenomenology of the Higgs Effective Lagrangian via FEYNRULES*, JHEP **04** (2014) 110, [arXiv:1310.5150 \[hep-ph\]](#).
- [5] C. Degrande, B. Fuks, K. Mawatari, K. Mimasu, and V. Sanz, *Electroweak Higgs boson production in the standard model effective field theory beyond leading order in QCD*, Eur. Phys. J. **C77** no. 4, (2017) 262, [arXiv:1609.04833 \[hep-ph\]](#).
- [6] J. Ellis, V. Sanz, and T. You, *The Effective Standard Model after LHC Run I*, JHEP **03** (2015) 157, [arXiv:1410.7703 \[hep-ph\]](#).
- [7] F. Ferreira, B. Fuks, V. Sanz, and D. Sengupta, *Probing CP-violating Higgs and gauge-boson couplings in the Standard Model effective field theory*, Eur. Phys. J. **C77** no. 10, (2017) 675, [arXiv:1612.01808 \[hep-ph\]](#).
- [8] M. E. Peskin and T. Takeuchi, *Estimation of oblique electroweak corrections*, Phys. Rev. **D46** (1992) 381.

- [9] The ALEPH, DELPHI, L3, OPAL, and SLD Collaborations, the LEP Electroweak Working Group, and the SLD Electroweak and Heavy Flavour Groups, *Precision electroweak measurements on the Z resonance*, Phys. Rep. **427** (2006) 257.
- [10] F. Krauss, S. Kuttimalai, and T. Plehn, *LHC multijet events as a probe for anomalous dimension-six gluon interactions*, Phys. Rev. **D95** no. 3, (2017) 035024, [arXiv:1611.00767](https://arxiv.org/abs/1611.00767) [hep-ph].
- [11] O. Domènech, A. Pomarol, and J. Serra, *Probing the standard model with dijets at the LHC*, Phys. Rev. D **85** (2012) 074030, [arXiv:1201.6510](https://arxiv.org/abs/1201.6510) [hep-ph].
- [12] “LHC Higgs XS WG / LHCXSWG2 / STXS · GitLab.”
<https://gitlab.cern.ch/LHCHIGGSXS/LHCHXSWG2/STXS>.
- [13] “STXStoEFT < LHCPhysics < TWiki .”
<https://twiki.cern.ch/twiki/bin/view/LHCPhysics/STXStoEFT>.
- [14] The ATLAS Collaboration, *Combined measurements of Higgs boson production and decay in the $H \rightarrow ZZ^* \rightarrow 4\ell$ and $H \rightarrow \gamma\gamma$ channels using $\sqrt{s} = 13$ TeV proton-proton collision data collected with the ATLAS experiment*, ATLAS-CONF-2017-047 (2017). <http://cdsweb.cern.ch/record/2273854>.
- [15] The ATLAS Collaboration, *Constraints on an effective Lagrangian from the combined $H \rightarrow ZZ^* \rightarrow 4\ell$ and $H \rightarrow \gamma\gamma$ channels using 36.1 fb^{-1} of $\sqrt{s} = 13$ TeV proton-proton collision data collected with the ATLAS detector*, ATLAS-PHYS-PUB-2017-018 (2017). <http://cdsweb.cern.ch/record/2293084>.
- [16] I. Brivio, Y. Jiang, and M. Trott, *The SMEFTsim package, theory and tools*, JHEP **12** (2017) 070, [arXiv:1709.06492](https://arxiv.org/abs/1709.06492) [hep-ph].
- [17] B. Grzadkowski, M. Iskrzynski, M. Misiak, and J. Rosiek, *Dimension-Six Terms in the Standard Model Lagrangian*, JHEP **10** (2010) 085, [arXiv:1008.4884](https://arxiv.org/abs/1008.4884) [hep-ph].
- [18] A. Falkowski, B. Fuks, K. Mawatari, K. Mimasu, F. Riva, and V. Sanz, *Rosetta: an operator basis translator for Standard Model effective field theory*, Eur. Phys. J. **C75** no. 12, (2015) 583, [arXiv:1508.05895](https://arxiv.org/abs/1508.05895) [hep-ph].
- [19] K. Mimasu, V. Sanz, and C. Williams, *Higher Order QCD predictions for Associated Higgs production with anomalous couplings to gauge bosons*, JHEP **08** (2016) 039, [arXiv:1512.02572](https://arxiv.org/abs/1512.02572) [hep-ph].

- [20] R. Contino, M. Ghezzi, C. Grojean, M. Mühlleitner, and M. Spira, *eHDECAY: an Implementation of the Higgs Effective Lagrangian into HDECAY*, Comput. Phys. Commun. **185** (2014) 3412–3423, [arXiv:1403.3381 \[hep-ph\]](#).

Table 3: The leading SM-EFT interference terms for each $gg \rightarrow H$, $qq \rightarrow Hqq$, and ttH cross section region for stage 1 of reference [3] relative to the SM (σ_i/σ_i^{SM}), at leading order in the SM EFT in the SILH basis. The equations are derived with the Madgraph generator and include showering with Pythia for determining the kinematic regions. For simplicity we only list Wilson coefficients whose pre-factor is $> 0.1\%$ times that of the leading pre-factor. Equations without this requirement will be available on the WG2 twiki.

Cross-section region	$\sum_i A_i c_i$
$gg \rightarrow H$ (0-jet)	
$gg \rightarrow H$ (1-jet, $p_T^H < 60$ GeV)	$56c'_g$
$gg \rightarrow H$ (1-jet, $60 \leq p_T^H < 120$ GeV)	
$gg \rightarrow H$ (1-jet, $120 \leq p_T^H < 200$ GeV)	$56c'_g + 18c3G + 11c2G$
$gg \rightarrow H$ (1-jet, $p_T^H \geq 200$ GeV)	$56c'_g + 52c3G + 34c2G$
$gg \rightarrow H$ (≥ 2 -jet, $p_T^H < 60$ GeV)	$56c'_g$
$gg \rightarrow H$ (≥ 2 -jet, $60 \leq p_T^H < 120$ GeV)	$56c'_g + 8c3G + 7c2G$
$gg \rightarrow H$ (≥ 2 -jet, $120 \leq p_T^H < 200$ GeV)	$56c'_g + 23c3G + 18c2G$
$gg \rightarrow H$ (≥ 2 -jet, $p_T^H \geq 200$ GeV)	$56c'_g + 90c3G + 68c2G$
$gg \rightarrow H$ (≥ 2 -jet VBF-like, $p_T^{j3} < 25$ GeV)	$56c'_g$
$gg \rightarrow H$ (≥ 2 -jet VBF-like, $p_T^{j3} \geq 25$ GeV)	$56c'_g + 9c3G + 8c2G$
$qq \rightarrow Hqq$ (VBF-like, $p_T^{j3} < 25$ GeV)	$-1.0cH - 1.0cT + 1.3cWW - 0.023cB - 4.3cHW$ $-0.29cHB + 0.092cHQ - 5.3cpHQ - 0.33cHu + 0.12cHd$
$qq \rightarrow Hqq$ (VBF-like, $p_T^{j3} \geq 25$ GeV)	$-1.0cH - 1.1cT + 1.2cWW - 0.027cB - 5.8cHW$ $-0.41cHB + 0.13cHQ - 6.9cpHQ - 0.45cHu + 0.15cHd$
$qq \rightarrow Hqq$ ($p_T^j \geq 200$ GeV)	$-1.0cH - 0.95cT + 1.5cWW - 0.025cB - 3.6cHW$ $-0.24cHB + 0.084cHQ - 4.5cpHQ - 0.25cHu + 0.1cHd$
$qq \rightarrow Hqq$ ($60 \leq m_{jj} < 120$ GeV)	$-0.99cH - 1.2cT + 7.8cWW - 0.19cB - 31cHW$ $-2.4cHB + 0.9cHQ - 38cpHQ - 2.8cHu + 0.9cHd$
$qq \rightarrow Hqq$ (rest)	$-1.0cH - 1.0cT + 1.4cWW - 0.028cB - 6.2cHW$ $-0.42cHB + 0.14cHQ - 6.9cpHQ - 0.42cHu + 0.16cHd$
$gg/q\bar{q} \rightarrow ttH$	$-0.98cH + 2.9cu + 0.93c'_g + 310cuG$ $+27c3G - 13c2G$

Table 4: The leading SM-EFT interference terms for each $q\bar{q} \rightarrow Hl\nu$ and $q\bar{q} \rightarrow Hll$ cross section region for stage 1 of reference [3] relative to the SM (σ_i/σ_i^{SM}), at leading order in the SM EFT in the SILH basis. The equations are derived with the Madgraph generator and include showering with Pythia for determining the kinematic regions.

Cross-section region	$\sum_i A_i c_i$
$q\bar{q} \rightarrow Hl\nu$ ($p_T^V < 150$ GeV)	$-1.0cH + 34cWW + 11cHW + 24cpHQ + 2.0cpHL$
$q\bar{q} \rightarrow Hl\nu$ ($150 \leq p_T^V < 250$ GeV, 0 jets)	$-1.0cH + 76cWW + 51cHW + 67cpHQ + 2.0cpHL$
$q\bar{q} \rightarrow Hl\nu$ ($150 \leq p_T^V < 250$ GeV, ≥ 1 jet)	$-1.0cH + 71cWW + 46cHW + 61cpHQ + 2.0cpHL$
$q\bar{q} \rightarrow Hl\nu$ ($p_T^V \geq 250$ GeV)	$-1.0cH + 200cWW + 170cHW + 190cpHQ + 2.0cpHL$
$q\bar{q} \rightarrow Hll$ ($p_T^V < 150$ GeV)	$-1.0cH - 4.0cT + 30cWW + 8.4cB + 8.5cHW$ $+2.5cHB + 0.032c_\gamma - 1.9cHQ + 23cpHQ + 5.2cHu$ $-2.0cHd - 0.96cHL + 2.0cpHL - 0.23cHe$
$q\bar{q} \rightarrow Hll$ ($150 \leq p_T^V < 250$ GeV, 0 jets)	$-1.0cH - 4.0cT + 62cWW + 18cB + 38cHW$ $+11cHB - 5.0cHQ + 61cpHQ + 14cHu - 5.2cHd$ $-0.98cHL + 2.1cpHL - 0.23cHe$
$q\bar{q} \rightarrow Hll$ ($150 \leq p_T^V < 250$ GeV, ≥ 1 jet)	$-1.0cH - 4.0cT + 58cWW + 17cB + 33cHW$ $+9.9cHB - 4.6cHQ + 56cpHQ + 14cHu - 4.6cHd$ $-0.99cHL + 2.1cpHL - 0.24cHe$
$q\bar{q} \rightarrow Hll$ ($p_T^V \geq 250$ GeV)	$-1.0cH - 4.0cT + 150cWW + 46cB + 130cHW$ $+38cHB - 14cHQ + 170cpHQ + 42cHu - 14cHd$ $-0.98cHL + 2.1cpHL - 0.24cHe$

Table 5: The leading beyond-SM EFT terms for each $gg \rightarrow H$ STXS region for stage 1 of reference [3] relative to the SM (σ_i/σ_i^{SM}), at leading order and in the SILH basis.

$gg \rightarrow H$ region	$\sum_{ij} B_{ij} c_i c_j$
0-jet	$780(c_g'^2 + c_g'^2) + c_g'(300cH + 1200cd + 700cuG - 200cdG + 200c3G)$
1-jet, $p_T^H < 60$ GeV	$780(c_g'^2 + c_g'^2) + c_g'(-1000cH - 1000cd - 2000cdG - 2000c2G) + c_g'(-2000tc3G)$
1-jet, $60 \leq p_T^H < 120$ GeV	$780(c_g'^2 + c_g'^2) + 70(tc3G^2 + c3G^2) + 80c2G^2 + c_g'(1000cH + 1000cd + 1000cuG + 3000cdG + 1000c3G - 1000c2G) + c_g'(2000tc3G)$
1-jet, $120 \leq p_T^H < 200$ GeV	$780(c_g'^2 + c_g'^2) + 940(c3G^2 + tc3G^2) + 560c2G^2 + 5.6cuG^2 + c_g'(2000cH + 4000cd + 4000cuG - 1000cdG + 1000c3G + 2000c2G) + c_g'(1000tc3G)$
1-jet, $p_T^H \geq 200$ GeV	$780(c_g'^2 + c_g'^2) + 32cuG^2 + 13100(c3G^2 + tc3G^2) + 12200c2G^2 + c_g'(8000cH - 14000cd - 4000cuG - 7000cdG - 6000c3G + 11000c2G) + c2G(800cH + 1200cu + 1300cuG + 1800cdG + 900cd + 2900c3G) + c3G(400cu + 100cd + 400cuG) + 10000c_g' tc3G$
≥ 2 -jet, $p_T^H < 60$ GeV	$780(c_g'^2 + c_g'^2) + 170(c3G^2 + tc3G^2) + 140c2G^2 + c_g'(-1000cH - 1000cd - 1000cuG - 1000cdG - 1000c3G + 2000c2G) + 2000c_g' tc3G + c3G(50c2G)$
≥ 2 -jet, $60 \leq p_T^H < 120$ GeV	$780(c_g'^2 + c_g'^2) + 360(c3G^2 + tc3G^2) + 410c2G^2 + c_g'(-2000cd - 1000cuG - 1000cdG - 2000c3G + 2000c2G) + c2G(-20cH - 20cu + 70c3G)$
≥ 2 -jet, $120 \leq p_T^H < 200$ GeV	$780(c_g'^2 + c_g'^2) + 1800(c3G^2 + tc3G^2) + 1900c2G^2 + c_g'(-1000cH - 2000cd - 1000cuG + 2000cdG - 2000c3G - 3000c2G) + c2G(-20cH - 20cu - 100cd + 40cuG - 110cdG + 340c3G) + c3G(10cH + 10cu + 30cd - 10cuG) + c_g'(3000tc3G)$
≥ 2 -jet, $p_T^H \geq 200$ GeV	$780(c_g'^2 + c_g'^2) + 63000c2G^2 + 35000(c3G^2 + tc3G) + c_g'(-1000cH - 3000cd - 4000cuG + 5000cdG - 9000c3G + 6000c2G) + c2G(-100cuG + 100cdG + 4500c3G) + c_g'(3000tc3G)$
≥ 2 -jet, VBF-like, $p_T^{j3} < 25$ GeV	$780(c_g'^2 + c_g'^2) + 240(c3G^2 + tc3G^2) + 360c2G^2 + c_g'(2000cH - 4000cd + 2000cuG + 2000cdG + 5000c3G + c2G(-20cH - 30cu + 10cuG + 30c3G) + c3G(-10cH + 20cu + 30cuG) + c_g'(4000tc3G)$
≥ 2 -jet VBF-like, $p_T^{j3} \geq 25$ GeV	$780(c_g'^2 + c_g'^2) + 540(c3G^2 + tc3G^2) + 950c2G^2 + c_g'(1000cH - 1000cd + 2000cuG - 1000cdG + 5000c3G + 3000c2G) + c2G(-70cH - 50cd - 80cu - 140cuG - 50cdG - 10c3G) + c3G(30cH + 20cu + 20cd + 30cuG + 20cdG) - c_g'(3000tc3G)$

Table 6: The leading beyond-SM EFT terms for two VBF kinematic regions for stage 1 of reference [3] relative to the SM (σ_i/σ_i^{SM}), at leading order in the SM EFT in the SILH basis. The equations are derived with the Madgraph generator and include showering with Pythia for determining the kinematic regions.

Cross-section region	$\sum_{ij} B_{ij} c_i c_j$
$qq \rightarrow Hqq$, VBF-like, $p_T^{j3} < 25$ GeV	$+0.25cH^2 + 1cT^2 + 6.8cWW^2 + 0.17cB^2 + 11cHW^2 + 0.21cHB^2 + 2.3cHQ^2$ $+11cPHQ^2 + 1.4cHu^2 + 0.97cHd^2 + 6.1cHud^2 + 3.9tcHW^2 + 0.07tcHB^2$ $+cH(0.52cT - 1.5cWW - 0.039cB + 2.3cHW + 0.15cHB - 0.029cHQ$ $+2.6cPHQ + 0.17cHu - 0.047cHd + 0.2cHud) + cT(-2cWW - 0.18cB$ $+1.9cHW + 0.59cHB - 0.18cHQ + 2.8cPHQ + 0.6cHu - 0.2cHd)$ $+cWW(0.52cB + 0.79cHW - 0.13cHB + 0.25cHQ + 0.44cPHQ + 0.094cHu$ $-0.2cHd + 0.25cHud - 0.17cuB - 0.099cuW - 0.052cdB + 0.11cdW)$ $+cB(0.19cHW + 0.074cHB - 0.13cHQ + 0.95cPHQ - 0.34cHu + 0.1cHd)$ $+cHW(1.4cHB - 0.26cHQ + 19cPHQ + 0.84cHu - 0.3cHd + 0.11cHud$ $+0.11cuB + 0.28cuW - 0.21cdB + 0.2cdW) + cHB(-0.085cHQ + 1.6cPHQ$ $+0.27cHu - 0.096cHd)$ $+cHQ(-0.53cPHQ - 0.025cHu + 0.078cHud + 0.085cuB + 0.028cuW + 0.026cdW)$ $+cPHQ(0.5cHu + 0.067cHd - 0.27cHud - 0.14cuB - 0.24cdB - 0.029cdW)$ $+cHu(-0.077cHd + 0.062cHud - 0.037cuW) + cHd(0.041cHud)$ $+cHud(0.1cuB + 0.089cuW + 0.063cdB + 0.048cdW) + tcHW(0.52tcHB)$
$qq \rightarrow Hqq$, VBF-like, $p_T^{j3} \geq 25$ GeV	$+0.25cH^2 + 1.1cT^2 + 7.7cWW^2 + 0.22cB^2 + 20cHW^2 + 0.38cHB^2 + 4cHQ^2$ $+20cPHQ^2 + 2.5cHu^2 + 1.6cHd^2 + 9.9cHud^2 + 6.7tcHW^2 + 0.13tcHB^2$ $+cH(0.53cT - 0.68cWW + 2.8cHW + 0.2cHB - 0.053cHQ + 3.4cPHQ$ $+0.22cHu - 0.087cHd + 0.1cHud) + cT(-1.4cWW + 0.037cB + 2.8cHW$ $+0.81cHB - 0.42cHQ + 3.5cPHQ + 0.86cHu - 0.32cHd - 0.14cHud)$ $+cWW(0.61cB + 7.7cHW + 0.07cHB + 0.32cHQ + 8.1cPHQ + 0.75cHu$ $-0.23cHd - 0.049cHud - 0.14cuB + 0.052cdB + 0.06cdW)$ $+cB(0.67cHW + 0.23cHB - 0.39cHQ + 1.5cPHQ - 0.28cHu + 0.13cHd$ $+0.066cHud) + cHW(2.5cHB - 0.75cHQ + 33cPHQ + 1.9cHu - 0.72cHd$ $-0.52cHud + 0.053cuB - 0.18cuW + 0.14cdB - 0.048cdW)$ $+cHB(-0.34cHQ + 2.4cPHQ + 0.58cHu - 0.16cHd)$ $+cHQ(-2cPHQ - 0.066cHu + 0.087cHd - 0.12cHud + 0.035cuW + 0.059cdW)$ $+cPHQ(1.1cHu - 0.34cHd - 0.25cHud + 0.25cuB - 0.096cuW + 0.13cdB$ $-0.25cdW) + cHu(0.071cHud + 0.042cuW - 0.034cdW) + cHud(-0.13cuB$ $+0.075cuW + 0.16cdB - 0.051cdW) + tcHW(0.84tcHB)$

Table 7: The leading beyond-SM EFT terms for two VBF kinematic regions for stage 1 of reference [3] relative to the SM (σ_i/σ_i^{SM}), at leading order in the SM EFT in the SILH basis. The equations are derived with the Madgraph generator and include showering with Pythia for determining the kinematic regions.

Cross-section region	$\sum_{ij} B_{ij} c_i c_j$
$qq \rightarrow Hqq$, $p_T^j \geq 200$ GeV	$+0.25cH^2 + 0.95cT^2 + 11cWW^2 + 0.22cB^2 + 12cHW^2 + 0.22cHB^2 + 2.9cHQ^2$ $+13cpHQ^2 + 1.6cHu^2 + 1.2cHd^2 + 7.3cHud^2 + 5.5tcHW^2 + 0.1tcHB^2$ $+cH(0.48cT - 1.9cWW - 0.057cB + 1.8cHW + 0.12cHB + 2.2cpHQ$ $+0.14cHu - 0.052cHd) + cT(-2.2cWW - 0.22cB + 1.6cHW$ $+0.47cHB - 0.031cHQ + 2.2cpHQ + 0.51cHu - 0.2cHd - 0.033cHud)$ $+cWW(0.91cB + 3.4cHW + 0.036cHB + 6.3cpHQ + 0.43cHu - 0.056cHd$ $+0.13cHud + 0.085cuB - 0.08cuW + 0.02cdB + 0.088cdW) + cB(0.42cHW$ $+0.12cHB - 0.18cHQ + 0.89cpHQ - 0.13cHu + 0.041cHd + 0.022cHud)$ $+cHW(1.5cHB - 0.058cHQ + 18cpHQ + 1cHu - 0.39cHd + 0.063cuB - 0.081cuW$ $+0.094cdW) + cHB(-0.078cHQ + 1.2cpHQ + 0.3cHu - 0.1cHd - 0.036cHud)$ $+cHQ(-0.72cpHQ - 0.054cHu + 0.029cHud)$ $+cpHQ(0.32cHu - 0.29cHd - 0.021cHud - 0.06cuB + 0.11cdB)$ $+cHu(-0.031cHd + 0.019cuB) + cHd(-0.024cHud)$ $+cHud(0.059cuB + 0.022cuW - 0.042cdB + 0.064cdW) + tcHW(0.73tcHB)$
$qq \rightarrow Hqq$, $60 \leq m_{jj} < 120$ GeV	$+5.4 \times 10^2 cWW^2 + 11cB^2 + 6.3 \times 10^2 cHW^2 + 12cHB^2 + 2.1 \times 10^2 cHQ^2$ $+7.5 \times 10^2 cpHQ^2 + 1.3 \times 10^2 cHu^2 + 75cHd^2 + 4.6 \times 10^2 cHud^2$ $+1.1 \times 10^2 tcHW^2 + 2.4tcHB^2 + cH(12cWW + 14cHW + 19cpHQ)$ $+cT(11cWW + 4.8cB + 16cHW + 4.8cHB - 2.3cHQ + 23cpHQ + 6cHu - 1.8cHd)$ $+cWW(69cB + 1 \times 10^3 cHW + 64cHB - 47cHQ + 1.2 \times 10^3 cpHQ + 80cHu$ $-26cHd - 3.2cHud - 1.9cdW)$ $+cB(68cHW + 20cHB - 17cHQ + 94cpHQ + 21cHu - 6.4cHd - 1.4cHud)$ $+cHW(83cHB - 52cHQ + 1.2 \times 10^3 cpHQ + 75cHu - 23cHd + 1.6cHud)$ $+cHB(-14cHQ + 87cpHQ + 22cHu - 7cHd)$ $+cHQ(-1.1 \times 10^2 cpHQ - 1.3cHu) + cpHQ(14cHu - 4.2cHd - 1.7cdB)$ $+cHu(-1.4cHd - 1.8cHud) + tcHW(15tcHB)$

Table 8: The leading beyond-SM EFT terms for a VBF kinematic region and ttH production for stage 1 of reference [3] relative to the SM (σ_i/σ_i^{SM}), at leading order in the SM EFT in the SILH basis. The equations are derived with the Madgraph generator and include showering with Pythia for determining the kinematic regions.

Cross-section region	$\sum_{ij} B_{ij} c_i c_j$
$qq \rightarrow Hqq$, rest	$+0.25cH^2 + 1cT^2 + 12cWW^2 + 0.3cB^2 + 30cHW^2 + 0.54cHB^2 + 6.1cHQ^2$ $+25cPHQ^2 + 3.5cHu^2 + 2.6cHd^2 + 16cHud^2 + 11tcHW^2 + 0.21tcHB^2$ $+cH(0.51cT - 0.79cWW + 3.1cHW + 0.22cHB - 0.1cHQ + 3cPHQ$ $+0.17cHu - 0.4cHud) + cT(-1.9cWW + 0.092cB + 2.4cHW + 0.82cHB$ $-0.18cHQ + 4cPHQ + 0.83cHu - 0.27cHd - 0.23cHud)$ $+cWW(1.4cB + 17cHW + 0.58cHB - 0.22cHQ + 19cPHQ + 0.73cHu$ $-0.37cHd - 0.35cHud - 0.07cuB - 0.41cuW - 0.29cdB - 0.29cdW)$ $+cB(1.3cHW + 0.39cHB - 0.49cHQ + 1.8cPHQ - 0.06cHu + 0.16cHd - 0.33cHud)$ $+cHW(3.6cHB + 0.12cHQ + 40cPHQ + 3.8cHu - 0.66cHd - 0.15cHud$ $+0.27cuB - 0.072cuW + 0.97cdB - 0.31cdW) + cHQ(-2.1cPHQ + 0.15cHu$ $+0.087cHd - 0.72cHud + 0.048cuB - 0.083cuW - 0.047cdW)$ $+cHB(-0.15cHQ + 2.8cPHQ + 0.67cHu - 0.29cHd) + tcHW(1.3tcHB)$ $+cPHQ(-0.2cHu + 0.17cHd - 0.33cHud + 0.36cuB - 0.46cdB + 0.15cdW)$ $+cHu(0.18cHd - 0.41cHud - 0.086cdW) + cHd(0.065cHud + 0.065cuW$ $+0.067cdW) + cHud(-0.09cuB - 0.065cuW - 0.24cdB + 0.24cdW)$
$gg/q\bar{q} \rightarrow ttH$	$120000cuG^2 + 140000(c3G^2 + tc3G^2) + 33000c2G^2 + 2.1cu^2$ $+cuG(110000c3G + 50000c2G + 400cu - 200cH) + c3G(-140000c2G)$

Table 9: The leading beyond-SM terms for each $q\bar{q} \rightarrow Hl\nu$ cross section region for stage 1 of reference [3] relative to the SM (σ_i/σ_i^{SM}), at leading order in the SM EFT in the SILH basis. The equations are derived with the Madgraph generator and include showering with Pythia for determining the kinematic regions.

Cross-section region	$\sum_{ij} B_{ij} c_i c_j$
$q\bar{q} \rightarrow Hl\nu,$ $p_T^V < 150$ GeV	$310c_{WW}^2 + 61c_{HW}^2 + 36t_{cHW} + 170c_{pHQ}^2 + 170c_{Hud}^2 + 1.1c_{pHL}^2$ $+c_H(-18c_{WW} - 6.1c_{HW} - 12c_{pHQ} - 1.0c_{pHL})$ $+c_{WW}(230c_{HW} + 460c_{pHQ} - 2.0c_{Hud} + 34c_{pHL})$ $+c_{HW}(170c_{pHQ} + 11c_{pHL}) + c_{pHQ}(24c_{pHL})$
$q\bar{q} \rightarrow Hl\nu,$ $150 \leq p_T^V < 250$ GeV, 0 jets	$1600c_{WW}^2 + 870c_{HW}^2 + 1200c_{pHQ}^2 + 1300c_{Hud} + 160t_{cHW}^2$ $+c_H(-33c_{WW} - 26c_{HW} - 26c_{pHQ} + 2200c_{HW})$ $+c_{WW}(2800c_{pHQ} + 3.0c_{Hud} + 88c_{pHL} + 7.0c_{uW} + 12c_{lW})$ $+c_{HW}(1900c_{pHQ} + 3.0c_{Hud} + 49c_{pHL}) - c_{Hud}(-4.0c_{pHL})$ $+c_{pHQ}(-5.0c_{Hud} + 68c_{pHL} + 4.0c_{uW} - 3.0c_{dW} + 6.0c_{lW})$
$q\bar{q} \rightarrow Hl\nu,$ $150 \leq p_T^V < 250$ GeV, ≥ 1 jet	$1500c_{WW}^2 + 800c_{HW}^2 + 1100c_{pHQ}^2 + 1200c_{Hud}^2 + 150t_{cHW}^2$ $+c_H(-29c_{WW} - 23c_{HW} - 35c_{pHQ}) + c_{Hud}(5.0c_{dW})$ $+c_{WW}(2000c_{HW} + 2600c_{pHQ} + 70c_{pHL} - 3.0c_{dW})$ $+c_{HW}(1800c_{pHQ} + 41c_{pHL}) + c_{pHQ}(65c_{pHL} - 4.0c_{uW} - 7.0c_{dW})$
$q\bar{q} \rightarrow Hl\nu,$ $p_T^V \geq 250$ GeV	$16000c_{WW}^2 + 14000c_{HW}^2 + 15000c_{pHQ}^2 + 16000c_{Hud}^2 + 520t_{cHW}^2$ $+c_H(-80c_{WW} - 70c_{HW} - 100c_{pHQ}) + c_{HW}(29000c_{pHQ} + 190c_{pHL})$ $+c_{WW}(30000c_{HW} + 32000c_{pHQ} + 70c_{Hud} + 210c_{pHL}) + c_{pHQ}(180c_{pHL})$

Table 10: The leading beyond-SM terms for two $q\bar{q} \rightarrow Hll$ cross section regions for stage 1 of reference [3] relative to the SM (σ_i/σ_i^{SM}), at leading order in the SM EFT in the SILH basis.

Cross-section region	$\sum_{ij} B_{ij} c_i c_j$
$q\bar{q} \rightarrow Hll$, $p_T^V < 150$ GeV	$4.0cT^2 + 240cWW^2 + 20cB^2 + 34cHW^2 + 3.0cHB^2 + 170cHQ^2 + 170cPHQ^2$ $+100cHu^2 + 75cHd^2 + 1.3cHL^2 + 1.3cPHL^2 + 26tcHW^2 + 2.3tcHB^2$ $+cH(2.0cT - 15cWW - 4.3cB - 4.4cHW - 1.3cHB + 1.0cHQ - 12cPHQ$ $-2.3cHu + 0.8cHd + 0.48cHL - 1.0cPHL) + cT(-59cWW - 17cB$ $-17cHW - 5.1cHB + 2.5cHQ - 46cPHQ - 11cHu + 3.7cHd + 1.9cHL$ $-4.1cPHL + 0.46cHe) + cWW(140cB + 150cHW + 44cHB + 0.5c_\gamma - 17cHQ$ $+390cPHQ + 82cHu - 31cHd - 14cHL + 33cPHL - 3.3cHe + 0.6cdB$ $+0.9cdW + 0.8c1B - 1.0c1W) + cB(42cHW + 12cHB - 2.8cHQ + 110cPHQ$ $+31cHu - 12cHd - 4.6cHL + 8.3cPHL - 1.2cHe) + cHW(20cHB - 5.3cHQ$ $+120cPHQ + 29cHu - 11cHd - 4.1cHL + 8.8cPHL - 0.8cHe) + cHB(-1.2cHQ$ $+37cPHQ + 8.8cHu - 3.5cHd - 1.2cHL + 2.6cPHL) + cHQ(-50cPHQ - 1.0cHd$ $+0.8cHL - 0.4cuB) + cPHQ(-1.0cHu - 0.6cHd - 12cHL + 24cPHL - 2.0cHe$ $+1.0cuB + 1.0cdW + 1.0c1B + 1.0c1W) + cHu(-2.3cHL + 4.9cPHL + 0.6cuB$ $+1.5cuW) + cHd(1.2cHL - 2.2cPHL) + cHL(-0.53cPHL) + tcHW(15tcHB)$
$q\bar{q} \rightarrow Hll$, $150 \leq p_T^V < 250$ GeV, 0 jets	$4.0cT^2 + 1000cWW^2 + 90cB^2 + 480cHW^2 + 43cHB^2 + 1200cHQ^2 + 12000cPHQ^2$ $+680cHu^2 + 490cHd^2 + 120tcHW^2 + 10tcHB^2 + cH(-24cWW - 9.0cB - 20cHW$ $-5.1cHB + 11cHQ - 25cPHQ - 11cHu + 2.0cHd + cT(-120cWW - 36cB$ $-75cHW - 22cHB + 13cHQ - 120cPHQ - 29cHu + 9.0cHd - 4.2cPHL)$ $+cWW(610cB + 1300cHW + 400cHB - 150cHQ + 2100cPHQ + 470cHu$ $-170cHd - 24cHL + 55cPHL + 7.0cuB + 10cuW + 14cdW + 30c1W)$ $+cB(380cHW + 110cHB - 39cHQ + 600cPHQ + 160cHu - 59cHd - 9.4cHL$ $+19cPHL - 2.2cHe) + cHW(290cHB - 78cHQ + 1300cPHQ + 320cHu - 110cHd$ $-18cHL + 41cPHL - 3.0cHe - 2.0cdB) + cHB(-21cHQ + 400cPHQ + 96cHu$ $-34cHd - 5.1cHL + 12cPHL) + cHQ(-380cPHQ + 30cHu + 2.0cHd + 14cHL$ $-6.0cHe + 25cuB + 24cdB + 10cdW - 3.0c1B + 4.0c1W) + cPHQ(10cHu$ $-40cHL + 80cPHL - 7.0cHe + 3.0cdW + 30c1B - 3.0c1W) + cHu(14cPHL$ $+3.0cHe - 8.0cuB + 8.0cdB + 8.0cdW + 13c1B + 7.0c1W)$ $+cHd(9.0cHL + 3.0cPHL - 4.0cuB - 3.0c1B - 6.0c1W) + tcHW(69tcHB)$

Table 11: The leading beyond-SM terms for two $q\bar{q} \rightarrow Hll$ cross section regions for stage 1 of reference [3] relative to the SM (σ_i/σ_i^{SM}), at leading order in the SM EFT in the SILH basis.

Cross-section region	$\sum_{ij} B_{ij} c_i c_j$
$q\bar{q} \rightarrow Hll,$ $150 \leq p_T^V < 250 \text{ GeV},$ $\geq 1 \text{ jet}$	$4.0cT^2 + 960cWW^2 + 82cB^2 + 440cHW^2 + 39cHB^2 + 1100cHQ^2 + 1100cpHQ^2$ $+640cHu^2 + 430cHd^2 + 110tcHW^2 + 9.7tcHB^2 + cH(2.1cT - 23cWW - 8.1cB$ $-18cHW - 4.9cHB - 36cpHQ - 2.0cHu) + cT(-110cWW - 34cB - 71cHW$ $-20cHB + 4.0cHQ - 120cpHQ - 24cHu + 10cHd + 2.0cHL - 4.2cpHL)$ $+cWW(560cB + 1200cHW + 340cHB - 200cHQ + 1900cpHQ + 440cHu$ $-150cHd - 24cHL + 68cpHL + 3.0cHe + 5.0cuB + 3.0cuW - 3.0cdB$ $-10cdW - 10c1W) + cB(330cHW + 100cHB - 30cHQ + 550cpHQ + 140cHu$ $-52cHd - 9.6cHL + 17cpHL - 2.3cHe) + cHW(260cHB - 120cHQ$ $+1200cpHQ + 290cHu - 100cHd - 20cHL + 29cpHL - 10cHe - 5.0cuB$ $+2.0cuW + 2.0cdB - 3.0cdW) + cHB(-30cHQ + 360cpHQ + 85cHu - 30cHd$ $-4.8cHL + 11cpHL) + cHQ(-420cpHQ - 20cHd + 17cHL + 23cHe + 3.0cuB$ $+17cuW + 6.0cdW + 30c1B + 10c1W) + cpHQ(-6.0cHd - 40cHL + 20cpHL$ $-20cHe + 10cuB - 10cuW - 3.0cdB + 10c1W) + cHu(-6.0cHL + 13cpHL$ $-3.0cHe + 10cuB + 4.0cdB + 10cdW + 4.0c1B) + cHd(-8.0cHL - 7.0cHe$ $-5.0cdB - 2.0c1B + 3.0c1W) + tcHW(65tcHB)$
$q\bar{q} \rightarrow Hll,$ $p_T^V \geq 250 \text{ GeV}$	$9600cWW^2 + 850cB^2 + 8000cHW^2 + 720cHB^2 + 14000cHQ^2 + 14000cpHQ^2$ $+8600cHu^2 + 5200cHd^2 + 380tcHW^2 + 35tcHB^2 + cH(-80cWW - 22cB$ $-50cHW - 90cpHQ - 30cHu) + cT(-310cWW - 90cB - 250cHW - 78cHB$ $-310cpHQ - 100cHu + 30cHd) + cWW(5700cB + 17000cHW + 5100cHB$ $-3200cHQ + 22000cpHQ + 5400cHu - 1700cHd - 70cHL + 160cpHL$ $-30cHe - 30cdW + 20c1B - 30c1W) + cB(5100cHW + 1500cHB - 880cHQ$ $+6400cpHQ + 1700cHu - 500cHd + 48cpHL) + cHW(4800cHB - 2900cHQ$ $+19000cpHQ + 4900cHu - 1500cHd - 50cHL + 130cpHL) + cHB(-870cHQ$ $+5700cpHQ + 1500cHu - 430cHd + 37cpHL) + cHQ(-6700cpHQ - 70cHu$ $+50cHd - 30cHL - 50cpHL - 40cuB - 30cdB - 30cdW - 30c1W)$ $+cpHQ(50cHd + 220cHL - 30cHe - 50cuB - 50cdW - 110c1B - 70c1W)$ $+cHu(-30cHL + 70cpHL - 20cuW - 30cdW) + cHd(30cHL + 40cHe$ $+tcHW(230tcHB)$

Table 12: The SM-EFT interference for the Higgs-boson partial widths relative to the SM (Γ_i/Γ_i^{SM}), at leading order in the SM EFT in the SILH basis. The total width $H \rightarrow \text{all}$ is evaluated by summing the individual listed processes.

Partial width	$\sum_i A_i c_i$
$H \rightarrow b\bar{b}$	$-1.0\text{cH} + 3.0\text{cd}$
$H \rightarrow WW^* \rightarrow l\nu l\nu$	$10\text{cWW} + 3.7\text{cHW} + 2.2\text{cpHL}$
$H \rightarrow ZZ^* \rightarrow 4l$	$55\text{cWW} + 13\text{cB} + 15\text{cHW} + 4.6\text{cHB} + 0.018c_\gamma + 2.0\text{cHL} + 2.0\text{cpHL} + 0.027\text{cHe}$
$H \rightarrow \gamma\gamma$	$-5.8c'_\gamma$
$H \rightarrow \tau\tau$	$-1.0\text{cH} + 3.0\text{c1}$
$H \rightarrow gg$	$56c'_g$
$H \rightarrow \text{all}$	$0.0029\text{cT} + 0.17\text{cu} + 2.3\text{cd} + 0.11\text{c1} + 1.0\text{cWW} + 0.023\text{cB} + 0.37\text{cHW}$ $+0.0079\text{cHB} + 1.6c'_g + 0.0078\text{cHQ} + 0.17\text{cpHQ} + 0.0027\text{cHu} + 0.057\text{cpHL}$

Table 13: The beyond-SM terms for the Higgs-boson partial widths relative to the SM (Γ_i/Γ_i^{SM}), at leading order in the SM EFT in the SILH basis. The total width $H \rightarrow \text{all}$ is evaluated by summing the individual listed processes.

Partial width	$\sum_{ij} B_{ij} c_i c_j$
$H \rightarrow b\bar{b}$	$0.25c_H^2 + 2.3cd^2 + c_H(-1.5cd)$
$H \rightarrow c\bar{c}$	$0.25c_H^2 + 2.3cu^2 + c_H(-1.5cu)$
$H \rightarrow \tau\tau$	$0.25c_H^2 + 2.3c_l^2 + c_H(-1.5c_l)$
$H \rightarrow \gamma\gamma$	$8.4(c_\gamma'^2 + c_\gamma^2)$
$H \rightarrow gg$	$790(c_g'^2 + c_g^2)$
$H \rightarrow WW^* \rightarrow l\nu l\nu$	$0.25c_H^2 + 26c_{WW}^2 + 3.8c_{HW}^2 + 1.3c_{pHL}^2 + 0.32t_{cHW}^2$ $+c_H(-5.1c_{WW} - 1.9c_{HW} - 1.1c_{pHL}) + c_{WW}(19c_{HW}) + 12c_{pHL}$ $+c_{HW}(4.3c_{pHL})$
$H \rightarrow ZZ^* \rightarrow 4\ell$	$0.25c_H^2 + 4.0c_T^2 + 28c_{WW}^2 + 3.5c_B^2 + 2.2c_{HW}^2 + 0.20c_{HB}^2 + 1.8c_{HL}^2$ $+1.8c_{pHL}^2 + 0.43c_{He}^2 + 0.14t_{cHW}^2 + c_H(2.0c_T - 5.1c_{WW} - 1.3c_B$ $-1.4c_{HW} - 0.43c_{HB} - 1.0c_{HL} - 1.0c_{pHL} + 0.43c_{He}) + c_T(-21c_{WW}$ $-5.3c_B - 5.7c_{HW} - 1.7c_{HB} - 4.1c_{HL} - 4.1c_{pHL} + 1.7c_{He}) + c_{WW}(10c_B$ $+15c_{HW} + 4.4c_{HB} + 12c_{HL} + 12c_{pHL} - 3.5c_{He}) + c_B(3.8c_{HW} + 1.1c_{HB}$ $+0.052c_\gamma' + 1.1c_{HL} + 1.1c_{pHL} - 2.1c_{He}) + c_{HW}(1.3c_{HB} + 3.0c_{HL}$ $+3.0c_{pHL} - 1.3c_{He}) + c_{HB}(0.91c_{HL} + 0.91c_{pHL} - 0.39c_{He})$ $+c_{HL}(3.5c_{pHL} - 0.13c_{He}) + c_{pHL}(-0.13c_{He}) + 0.081t_{cHW}(t_{cHB})$
$H \rightarrow \text{all}$	$0.24c_H^2 + 0.037c_T^2 + 0.13cu^2 + 1.7cd^2 + 0.084c_l^2 + 2.6c_{WW}^2 + 4.7c_{HW}^2$ $+4.3c_{HB}^2 + 23c_g'^2 + 0.09c_{pHQ}^2 + 0.066c_{Hud}^2 + 0.027c_{pHL}^2 + 4.3t_{cHW}^2$ $+4.3t_{cHB}^2 + 23c_g^2 + c_H(-0.086cu - 1.2cd - 0.056c_l - 0.51c_{WW}$ $-0.18c_{HW} - 0.083c_{pHQ} - 0.029c_{pHL}) + c_T(-0.19c_{WW} - 0.046c_B$ $-0.051c_{HW} - 0.027c_{pHQ}) + c_{WW}(0.11c_B + 1.9c_{HW} + 0.04c_{HB} + 0.86c_{pHQ}$ $+0.29c_{pHL}) + c_{HW}(0.03c_B - 8.6c_{HB} + 0.1c_\gamma + 0.31c_{pHQ} + 0.11c_{pHL})$ $+c_{HB}(-0.1c_\gamma) + t_{cHW}(-8.6t_{cHB} + 0.1c_\gamma') + t_{cHB}(-0.10c_\gamma')$